Thermodynamic and Structural Effect of Urea and Guanidine Chloride on the Helical and on a Hairpin fragment of GB1 from Molecular Simulations

R. Meloni and G. Tiana*

Center for Complexity and Biosystems and Department of Physics, Università degli Studi di Milano and INFN, via Celoria 16, 20133 Milano, Italy

Short title: Simulation of GB1 fragments in urea and guanidine chloride

Keywords: denaturants, metadynamics, MD simulations, circular dichroism, chemical shifts, m-value

*** Correspondence to**:

Guido Tiana, Center for Complexity and Biosystems and Department of Physics, Università degli Studi di Milano and INFN, tel. +39-0250317221, email: guido.tiana@unimi.it

Abstract

With the help of molecular-dynamics simulations, we studied the effect of urea and guanidine chloride on the thermodynamic and structural properties of the helical fragment of protein GB1, comparing them with those of its second beta hairpin. We showed that the helical fragment in different solvents populates an ensemble of states that is more complex than that of the hairpin, and thus the associated experimental observables (circular-dichroism spectra, secondary chemical shifts, *m*-values), that we back-calculated from the simulations and compared with the actual data, are more difficult to interpret. We observed that in the case of both peptides, urea binds tightly to their backbone, while guanidine exerts its denaturing effect in a more subtle way, strongly affecting the electrostatic properties of the solution. This difference can have consequences in the way denaturation experiments are interpreted.

Introduction

The study of the disordered phases of proteins and peptides is an important, although complicated, task. The denatured state of structured proteins is critical for determining their folding kinetics and thermodynamic stability, their ability to cross lipid bilayers, and their turnover in the cell[1]. In the case of intrinsically disordered proteins, disordered states are directly involved in biological function [2].

Fluorescence and circular-dichroism (CD) spectroscopy provide coarse information about non-native states. NMR techniques can refine it to the amino-acid length-scale. However, for structured proteins the conformational characterization of the denatured state requires its stabilization, typically with denaturants like urea or guanidine chloride[3] (GndCl). The natural question one is pushed to ask is then what is the effect of these denaturants on the thermodynamic and structural properties of the polypeptide chain. In particular, one is usually interested in the properties of the (metastable) denatured state in water, that is under chemical conditions that are more similar to the biological ones. Thus, studying the effect of chemical denaturants can be relevant for interpreting the results of experiments conducted in urea or GndCl, in order to extrapolate information on the biological denatured state.

The mechanism that allows urea and GndCl to stabilize the denatured state of proteins has been discussed for forty years. The particularly low viscosity of urea solutions raised the suggestion that it affects the hydrogen bonding of the water, decreasing the effective hydrophobic interaction that stabilizes proteins[4]. Although this could be the case, calorimetric experiments suggest that the main

factor that destabilizes the native state of proteins is a direct interaction with the denaturant molecules[5]. Also molecular dynamics simulations point towards a direct interaction of chemical denaturants with the protein backbone[6-8]. Hydrogen-exchange experiments indicate that urea can interact with the protein, building hydrogen bonds (mainly) with its backbone, but no relevant hydrogen bonds are detected in the case of GndCl[9]. Thus, urea and GndCl seem to act according to different mechanisms.

This fact has consequences on the kinetics of protein chains. The different viscosity and association propensity to a poly-dipeptide was shown to be the cause of the dissimilar rate constants of the end-to-end diffusion in urea and GndCl[10]. Unfolding simulations of protein L in these two denaturants highlighted a different order in the disruption of its secondary structure elements[11].

Different denaturants are then expected to have distinct effects in determining the non-native states of proteins. This is apparent in the case of GB1, one of the most widely characterized proteins with biochemical techniques. GB1 follows a two state behavior in urea[12,13] but it displays an intermediate in GndCl[14,15]. From the structural point of view, GB1 shows essentially no residual secondary structure in 7.4M urea[12], while in GndCl its second hairpin has some residual structure[14]. The scenario is still different if GB1 is denatured by mutating an amino acid and lowering the pH, thus under conditions expectedly closer to the biological (metastable) denatured state[16].

In order to investigate the molecular effect of the chemical denaturant on proteins, we carried out molecular dynamics simulations of the helical segment and of the second hairpin of GB1 in urea and GndCl at equilibrium, and we compared them with simulations conducted in water.

The same fragments of GB1 were characterized experimentally by circular dichroism and NMR. Fragment 41-56, corresponding to the second hairpin was shown to be structured in water[17]. Upon addition of 6M urea, it still retains 40% native population[18]. The fragment 21-40, corresponding to the central helix of the protein, is mainly unstructured in water, but its CD spectrum further shifts towards random-coil values if 6M urea is added. Nuclear Overhauser Effect signals indicate that in water its N-terminal region populates the beta region of dihedral space, while the C-terminal is in the alpha region[18]. The residual helical population, estimated from its ellipticity, is 9% [19].

A large number of simulations were described in the literature to investigate the equilibrium properties of the fragment corresponding to the second hairpin of GB1 in water [20-23], to the extent that it has become the sand box to test routinely new algorithms. According to all these calculation, this fragment displays a clean two-state behavior in water. The equilibrium sampling of the fragment corresponding to the alpha-helix of GB1 in water highlights a more complicated free-energy landscape[24], in which the metastable alpha-helix competes not only with a random-coil state, but also with other types of helices and with a hairpin state.

The comparison of the free-energy landscapes of the hairpin fragment of GB1 in urea, GndCl and water was reported on the basis of Hamiltonian-exchange simulations[25]. According to these calculations, urea disrupts completely the native region and stabilizes a state that resembles a random coil, while guanidine chloride has a milder effect, maintaining the structure the peptide has in water. A random-coil behavior in urea was also found in parallel-tempering metadynamics simulations[8].

In the present work, we simulated the fragment corresponding to the helix of GB1 in water, urea and GndCl, comparing the associated free-energy landscapes, and we studied the interaction between the solvent and the peptide. Moreover, we extended our previous calculations concerning the fragment corresponding to the second hairpin fragment of GB1[25] to study also in this case the interactions between the peptide and the denaturant.

Materials and Methods

The segment 22-38 of GB1 (pdb code 1PGB) was modeled with the Amber99 potential, as modified in ref. 26. The parameters for urea were those of Amber99, while those for GndCl were those developed in ref. 11. The model for segment 41-56 is identical to that reported previously[25].

The simulations were carried out with the bias-exchange metadynamics algorithm[27], implemented in Plumed 2 [28] for Gromacs 5.0.

A total of five different environmental conditions was studied for the α-helix: in pure water, or in a solution with 2M urea, 5M urea, 2M GndCl or 4M GndCl; the β–hairpin was instead simulated in three cases: in pure water or in a solution with 5M urea or 4M GndCl. Initially, both the α-helix and the β-hairpin were unfolded at 800 K, in aqueous environment. The unfolded structures were then inserted in a dodecahedric box (of volumes Vα=85 nm^3 and Vβ=88 nm^3) and solvated with:

(α-helix) 98 or 245 molecules of urea (corresponding to ~2M and ~5M respectively), 98 or 196 molecules of Gnd^- (~2M and ~4M),

(β-hairpin) 265 molecules of urea (~5M) or 200 molecules of Gnd^- (~4M).

Tip3p-water molecules were used to fill the remaining empty volume; ions Na^+ and Cl^- were finally added to ensure charge neutrality. After a 5ns equilibration run in NVT regime, simulations were carried out at T=300 K, coupled with a v-rescale thermostat (τ=0.1 ps); electrostatic interaction was evaluated with PME algorithm; an integration timestep Δt=2 fs was used, keeping the bond lengths constant via LINCS algorithm.

Each of the eight systems was structured in a five-replicas, bias-exchange well-tempered metadynamics scheme: the first replica was biased along the degree of helicity $R\alpha$[29], the second one along the degree of β-content $R\beta$[29], the third one on the radius of gyration R_g and the fourth one on the end-to-end distance d_{ee}; the fifth replica was left unbiased. Exchanges were attempted every 50 ps; the hills used had height=0.3 kJ/mol and width=0.2 for all CVs, deposited every 500 timesteps with a biasfactor=10. Each replica was run for 2μs.

The CD spectrum was predicted as a linear combination of the standard spectra[30], weighted by the probabilities of α, β and coil structures calculated with STRIDE[31] on the unbiased replica.

The chemical shifts were calculated using SPARTA[32] on the nine conformations displayed in Fig. 1 and weighted by their Boltzmann factor evaluated in terms of $R\alpha$, $R\beta$ and R_g.

Results

The effect of urea and GndCl on the states of fragment 22-38

Five simulations of the fragment 22-38, corresponding to the helix of GB1, were carried out in water, 2M urea, 5M urea, 2M GndCl and 4M GndCl, respectively,

until convergence (cf. Figs. S1-S2 in the Supplementary Materials). The free energy profile of this fragment in water, as a function of the helicity $R\alpha$ and of the gyration radius R_g, is displayed in the left panel of Fig. 1. Its features are in agreement with those calculated previously[24], namely a metastable helical state ~5kT above the random coil, and a variety of local minima corresponding to different degree of formation of the helix, including a partially-formed β-hairpin state (cf. also Fig. S3 in the Supplementary Materials, where the free energy is showed as a function of $R\beta$ and R_g).

In the free-energy profile we identified nine local minima separated by at least *kT=2.5 kJ/mol* from the surrounding. The minima are marked with crosses, and some of the associated conformations are plotted in the figure. The peptide does not exhibit a clear two-state behavior, in agreement with the Zimm-Bragg theory[33]. Besides the fully formed helix (labelled as H1), there are other two states in the region $R\alpha \geq 0.5$ in which only the C-terminus is helical. In the other half of the plot one can identify at least five disordered states with varying gyration radius, and the β-hairpin.

In the right panels of Fig. 1 we show how the free-energy landscape is changed upon addition of 5M urea and 4M GndCl, respectively (landscapes in milder denaturing conditions are displayed in Fig. S4 in the Supplementary Materials). Urea has the strongest effect on the helical state; the fully formed helix (H1) is lost, while the free energy of states H2 and H3 is raised of $12kT$ and $5kT$, respectively. Also the free energy of coil states at intermediate values of $R\alpha$ is raised of several kT. The global minimum is squeezed towards the value $R\alpha \approx 0$,

and it is rather flat at values of R_g between 0.6 and 1.4 nm. Also the hairpin state B1 essentially disappears (cf. Fig. S5 in the Supplementary Materials).

Guanidine chloride has a smaller effect on the peptide. The free energy of the helical state H1 is raised by 5*kT*, and the rest of the landscape at $R\alpha>0$ is raised by few *kT*, maintaining a pattern of local minima similar to that in water. Also the β-hairpin state B1 is raised by some *kT* but it is still detectable (cf. Fig. S5 in the Supplementary Materials).

Experimental observables associated with fragment 22-38

From the ensemble of conformations generated by the simulation, one can calculate some macroscopic observables and compare them with those measured in experiments. Moreover, one can use these data to evaluate if their interpretation according to the standard view is compatible with the underlying conformational properties of the peptide, given by the model calculations.

In Fig. 2a we reported the CD spectrum of the peptide in the five simulated solutions. Similarly to the experimental findings[19], the curves recorded in water and at high urea concentration (6M in the experiment, 5M in the simulations) are similar, the latter displaying an upward shift in the region around 220 nm. Overall, the curve in water is very similar to that in 2M GndCl; the curve in 4M GndCl is similar to that in 2M urea, displaying a more pronounced minimum at 195 nm, and this minimum decreases even more at 5M urea.

The secondary-structure profiles, calculated from the same ensemble of conformations used to predict the CD spectra, are displayed in Fig. 3. Under all conditions the helicity is concentrated in the C-terminal half of the peptide, in agreement with the corresponding sequence-based propensities[19]. The overall

helicity of the peptide is comparable in water and in 2M GndCl, and decreases moving to 2M urea, 4M GndCl and reached its minimum at 5M urea. On the other hand, a residual β-structure is apparent in water, but diminishes in all the other denaturants.

Analysis of CD spectra associated with residual secondary structure is always cumbersome. The complexity of the conformational space of the fragment 22-38 makes its interpretation even worse. All the curves are dominated by the coil component. The similarity between the curves in water and 2M GndCl and between those in 2M urea and 4M GndCl actually derives from different combination of α and β components. Indeed the de-convolution of the predicted CD spectra with different standard tools gives different secondary-structure propensities (cf. Table S1 in the Supplementary Materials).

Also the secondary chemical shifts predicted from the simulation and displayed in Figs. 2b, c and d display a complex behavior that makes their interpretation uneasy. In pure water, the CA chemical shifts are positive in the regions 23-26 and 32-34 and at residue 29, that usually indicates helical behavior, while they are null or negative in the central region. This interpretation does not correspond to the actual population of secondary structures, displayed in Fig. 3. In fact, the positive chemical shifts induced by the helical population, especially in the C-terminal region, is counterbalanced around residues 27 and 33 by the β–hairpin population, that contributes with negative chemical shifts. A similar trend is followed by the HA chemical shifts, although here signs are reversed (for HA it is negative chemical shifts to indicate helical behavior). The dependence of the chemical shifts on the type and concentration of denaturant is quite irregular,

due to the irregular contribution of β structure in compensating that of the helical population, which vice versa is quite regular (cf. Fig. 3).

The secondary chemical shifts associated with the CB are markedly positive, indicating only β content, in contrast to what suggested by the signals from CA and HA. This is probably due to a failure of random-coil referencing[32] for our peptide. In fact, a downshift of ~1 ppm of all CB chemical shifts would result in data that are grossly consistent with CA and HA, although again not easy to interpret from a structural point of view.

Two-state approximation and m-values

Chemical denaturation is often described assuming a two state model and a linear dependence of the free energy difference between the two states on the concentration of denaturant[34], according to

$$\Delta F([D]) = \Delta F - m[D] \quad (1)$$

where ΔF is the free energy difference in water, $[D]$ is the concentration of denaturant and m is the proportionality constant. Usually, ΔF and m are obtained by a fit of the native probability p_N, obtained by fluorescence or CD, as a function of $[D]$, following $p_N = exp\left[\frac{-\Delta F([D])}{kT}\right] / \left(1 + exp\left[\frac{-\Delta F([D])}{kT}\right]\right)$. However, in the present case we have only three points for each denaturant, and thus the non-linear fit is unfeasible. Consequently, we defined the native state on the basis of the free-energy profile of Fig. 1 as $R\alpha > 0.5$, including states H1, H2 and H3. The corresponding free energies differences $\Delta F([D])$ are displayed in Fig. 4a. The curves are rather linear, and thus are in agreement with Eq. (1) with m-values 3.23 kJ/mol/M for GndCl and 2.88 kJ/mol/M for urea. The value in GndCl

is larger than that in urea, as typically found in the literature[34]. However, one should notice that the two-state picture gives only a partial picture of the effect of the denaturants. As shown in Fig. 1 (and Fig. S4 in the Supplementary Materials), urea has a stronger effect in destabilizing the fully formed helix (state H1) than GndCl; vice versa, GndCl has a stronger effect in destabilizing the partially formed helices H2 and H3. This rearrangement of the probability distribution within the native state is lost in the two-state approximation. One should also notice that other definitions of the native state do not lead to a linear dependence of ΔF on $[D]$ (see Fig. S6 in the Supplementary Materials).

In the case of urea, the linear change in free energy corresponds to a linear change in the solvent accessible surface area (SASA), as displayed in Fig. 4b. The free-energy gain per area in urea is approximately 7 kJ/mol/nm^2. This behavior is in agreement with the classical model of protein denaturation[35]. The effect of GndCl on the SASA is different, and the exposed area saturates at about 18 nm^2, corresponding to conformations more compact than those denatured by urea (cf. also Fig. 1). A detailed comparison of the equilibrium SASA per-residue under different conditions is displayed in Fig. 4c. The SASA in urea are systematically larger for each residue than in water. On the other hand, in GndCl the SASA is more similar to that in water, except for GLU27, LYS28 and ASP36, that are charged residues.

Distribution of the solvent around fragment 22-38

The distribution of solvent around the peptide was investigated inspecting the radial distribution functions (rdf) of water and of denaturant molecules as a function of their minimum distance from any atom of each amino acid of the

peptide. Two typical behaviors were found and illustrated in Fig. 5, where the rdf associated with ALA26 and GLU27 are displayed (those associated with the other amino acids are displayed in Fig. S7 of the Supplementary Materials).

The shape of the rdf of water molecules is approximately the same for all residues (cf. Fig. 5a and c). In presence of urea, the distribution of water molecules in the first shell around the residue (labeled as region S_1 in Fig. 5c) is much depleted. Vice versa, in presence of GndCl the density of water in region S_1 is weakly affected, and sometimes is even increased in 4M GndCl. In the second shell of water molecules (labeled as region S_2 in Fig. 5c), the density is decreased in presence of urea and is unaffected in presence of GndCl at any concentration.

The rdf of denaturant molecules, either urea or GndCl, is more residue-dependent. For most residues the rdf of denaturant is that displayed in Fig. 5b. The density of urea is largely enriched in region S_1 with respect to water and there is a marked peak in region S_2 whose height is comparable with the density of water, but anyhow higher than the bulk density of urea. The rdf of Gnd displays peaks both in regions S_1 and S_2, in both cases lower than the corresponding density of water.

Two residues display a different rdf for Gnd (see Fig. 5d), displaying a much higher peak in region S_1 and essentially no peak in S_2. They are GLU27 and ASP36 which, not unexpectedly, are the two displaying a negative charge.

The picture that emerges is that urea binds directly to the peptide, displacing water molecules, but GndCl binds it to a much smaller extent. Thus, to investigate more the effect of GndCl on the stability of the peptide we focused on its electrostatic, long-range properties.

The fully formed helix has a dipole moment μ=158 D (see Fig. 6a), which decreases to ~90 D as the helix is disrupted into a coil (see Fig. 6b). The dipole induces a separation of Gnd+ and Cl- ions which, in turn, produces an electric potential on the helix (see color distribution in Fig. 6a). The separation of charges, besides being favorable from the point of view of the balance between Coulomb interaction and demixing entropy, gains Lennard-Jones energy between Gnd ions (see Fig. S8 in the Supplementary Materials), presumably associated with hydrogen bonding between Gnd groups[36]. The result is a minimum in the free energy of the system when the dipole associated with the helix assumes minimum modulus (cf. Fig. 6b with Fig. 1 and Discussion section below).

Comparison with the denaturation of hairpin fragment

We studied the free energy profile of the second hairpin of GB1 (fragment 41-56) in water, 4M GndCl and 5.5M urea in a previous article[25]. The result was that the peptide is stable in water at 300K, displaying a partially-native intermediate. Urea disrupts completely the native region and stabilizes a state that resembles a random coil, while guanidine chloride has a milder effect, also maintaining the intermediate state.

Here we analyze the properties of the solvent around the molecule to investigate the molecular mechanism of denaturation. In Fig. 7a-d we display the rdf of water and denaturant around ALA26 and GLU27 (the others are in Fig. S9 in the Supplementary Materials). Differently from the helix, water molecules in the simulation of the hairpin in GndCl experiences a modification both in the first and in the second shell, most notably around GLU42, ALA48, THR49, LYS50,

THR55. The accumulation of Gnd is observed here not only around negatively-charged residues, but also around polar residues as ASN35 and ASN37.

Also the native hairpin displays an electric dipole, but its modulus is 100 D, smaller than that of the helix, and consequently the charge separation in solution is also more limited (cf. Fig. 7e).

Experimental observables concerning the hairpin fragment

The relatively simpler structure of the free-energy profile of the hairpin fragment with respect to the helical fragment makes the interpretation of associated experimental observables potentially simpler. Fig. 8 displays the CD spectrum and the secondary chemical shifts predicted by the simulations for the hairpin in water and in denaturants. The CD spectrum reports a clean β structure in water, that becomes more coil-like in GndCl and urea.

The secondary chemical shifts (see Fig. 8b, c, d) in water are consistent with a β–hairpin, with negative values for CA and positive values for CB and HA towards the termini. Under denaturing conditions, the picture becomes more involved. For example, in 5M urea the peptide is essentially coil, but the secondary chemical shifts of all atoms (blue striped bars in Fig. 8) display an irregular behavior.

The *m*-value resulting from the simulations of the hairpin fragment is 4.0 kJ/mol/M for urea and 1.8 kJ/mol/M for GndCl, displaying in this case a larger value for urea.

Discussion

The helix and the second hairpin of GB1 are among the most studied small peptides in the literature, both from an experimental and a computational point of view.

As in the case of larger proteins, a standard experimental tool to probe the thermodynamic and conformational properties of these peptides is to denature them with urea or GndCl. However, the result of these experiments can be difficult to interpret, or even tricky. Simulations performed with advanced sampling techniques can be useful to rationalize the raw experimental data and to monitor quantities that are difficult to access in experiments.

In the specific case of the two fragments of GB1, the data on hairpin at 300K are rather simple to interpret. Its conformational space in water displays three well-defined states corresponding to the fully formed, to the half formed hairpin, and to a random coil. The effect of chemical denaturants is to decrease the population of the native state, without changing the structure of the conformational space. At 300K the population of helical states is negligibly low. Consequently, experimental observables like CD spectra and secondary chemical shifts just report the fraction of β-content of the peptide. Their main limitation is that they cannot distinguish between the fully formed helix populated with probability one half and the half-formed helix populated with probability one.

The situation for the helix is more complex. Several states, involving different degrees of structures α and β, compete with each other. The experimental data are the sum of the contributions of all these states. This is particularly problematic in the case of secondary chemical shifts, in which α and β give

contributions with opposite sign, reporting a random-coil behavior when α and β states have comparable probabilities.

The effect of urea appears rather simple from the simulations. It fills the first shell of solvent around the peptides in a residue-independent way, thus breaking the hydrogen bonds, that are the main interactions that stabilize either the helix or the hairpin. This is the reason why urea is so effective in stabilizing the denatured state of short peptides, containing only secondary structure, as compared with GndCl. In fact, in the case of full proteins, also stabilized by tertiary interactions, the denaturant power of urea is usually comparatively smaller[34]. This picture is in agreement with the results of hydrogen-exchange NMR experiments, which show that urea, but not GndCl, can form hydrogen bonds with peptides[9].

In fact, the denaturing mechanism of GndCl seems more complex. To some extent, Gnd accumulates in the neighborhood of the peptides, at various distances from its surface and differently for each type of amino acids. As expected, the effect is very large for acid residues and negligible for basic residues. As a rule, it does not seem to deplete the concentration of water in the first shell or to modify its rdf appreciably.

Another effect of GndCl is to generate an electric field that interacts with the electric dipole of the peptide. This effect is very clear for the helix, that has a large dipole moment due to the spatial alignment of its amino acids, and is smaller for the hairpin, in which the (smaller) dipole moment is due to the specific sequence of acid and basic residues (42E, 46D, 47D, 50K, 56E). The modulus of the electric dipole depends on the degree of formation of the secondary structure. In presence of GndCl, each of the effective charges that

define the dipole is screened by ions of opposite charge. Thus, the two of them undergo a screened attractive Coulomb interaction that tends to decrease their (effective) distance and then to decrease the modulus of the dipole moment. The equilibrium state corresponds then to a small dipole, and thus to a denatured peptide.

References

1. Dill KA, Shortle D. Denatured states of proteins. Annu Rev Biochem. 1991;60:795–825.

2. Uversky VN. Natively unfolded proteins: a point where biology waits for physics. Protein Sci. 2002;11:739–56.

3. Shortle D. The denatured state (the other half of the folding equation) and its role in protein stability. The FASEB Journal. 1996;10:27–34.

4. Rupley JA. The Effect of Urea and Amides upon Water Structure. J Phys Chem; 1964;68:2002–3.

5. Makhatadze GI, Privalov PL. Protein interactions with urea and guanidinium chloride. A calorimetric study. J Mol Biol. 1992;226:491–505.

6. O'Brien EP, Dima RI, Brooks B, Thirumalai D. Interactions between hydrophobic and ionic solutes in aqueous guanidinium chloride and urea solutions: lessons for protein denaturation mechanism. J Am Chem Soc. 2007;129(23):7346–53.

7. Stumpe MC, Grubmüller H. Interaction of urea with amino acids: implications for urea-induced protein denaturation. J Am Chem Soc. 2007;129:16126–31.

8. Berteotti A, Barducci A, Parrinello M. Effect of urea on the β-hairpin conformational ensemble and protein denaturation mechanism. J Am Chem Soc. 2011;133:17200–6.

9. Lim WK, Rösgen J, Englander SW. Urea, but not guanidinium, destabilizes proteins by forming hydrogen bonds to the peptide group. Proc Natl Acad Sci USA. 2009;106:2595–600.

10. Möglich A, Krieger F, Kiefhaber T. Molecular basis for the effect of urea and guanidinium chloride on the dynamics of unfolded polypeptide chains. J Mol Biol. 2005;345:153–62.

11. Camilloni C, Rocco AG, Eberini I, Gianazza E, Broglia RA, Tiana G. Urea and guanidinium chloride denature protein L in different ways in molecular dynamics simulations. Biophys J. 2008;94:4654–61.

12. Frank M, Clore G, Gronenborn A. Structural and dynamic characterization of the urea denatured state of the immunoglobulin binding. Protein Sci. 1995;4:2605–15.

13. Chung HS, Louis JM, Eaton WA. Experimental determination of upper bound for transition path times in protein folding from single-molecule photon-by-photon trajectories. Proc Natl Acad Sci USA. 2009;106:11837–44.

14. Kuszewski J, Clore GM, Gronenborn AM. Fast folding of a prototypic polypeptide: the immunoglobulin binding domain of streptococcal protein G. Protein Sci. 1994;3:1945–52.

15. Tcherkasskaya O, Knutson JR, Bowley SA, Frank MK, Gronenborn AM. Nanosecond dynamics of the single tryptophan reveals multi-state equilibrium unfolding of protein GB1. Biochemistry. 2000;39:11216–26.

16. Sari N, Alexander P, Bryan P, Orban J. Structure and dynamics of an acid-denatured protein G mutant. Biochemistry. 2000;39:965-967.

17. Blanco FJ, Rivas G, Serrano L. A short linear peptide that folds into a native stable beta-hairpin in aqueous solution. Nat Struct Biol. 1994;1:584–90.

18. Blanco F, Serrano L. Folding of Protein G B1 Domain Studied by the Conformational Characterization of Fragments Comprising its Secondary Structure Elements. FEBS J. 1995; 230:634-649

19. Blanco FJ, Ortiz AR, Serrano L. Role of a nonnative interaction in the folding of the protein G B1 domain as inferred from the conformational analysis of the alpha-helix fragment. Folding and Design. 1997;2:123–33.

20. Bussi G, Gervasio FL, Laio A, Parrinello M. Free-energy landscape for beta hairpin folding from combined parallel tempering and metadynamics. J Am Chem Soc. 2006;128:13435–41.

21. Bonomi M, Branduardi D, Gervasio F, Parrinello M. The Unfolded Ensemble and Folding Mechanism of the C-Terminal GB1 β-Hairpin. J Am Chem Soc. 2008;130:13928.

22. Best RB, Mittal J. Free-energy landscape of the GB1 hairpin in all-atom explicit solvent simulations with different force fields: Similarities and differences. Proteins. 2011;79:1318–28.

23. Capelli R, Villemot F, Moroni E, Tiana G, van der Vaart A, Colombo G. Assessment of Mutational Effects on Peptide Stability through Confinement Simulations. J Phys Chem Lett. 2016;7:126–30.

24. Camilloni C, Provasi D, Tiana G, Broglia RA. Exploring the protein G helix free-energy surface by solute tempering metadynamics. Proteins. 2008;71:1647–54.

25. Meloni R, Camilloni C, Tiana G. Sampling the Denatured State of Polypeptides in Water, Urea, and Guanidine Chloride to Strict Equilibrium Conditions with the Help of Massively Parallel Computers.J. Chem. Theo. Comp. 2014;10:846–54.

26. Best RB, De Sancho D, Mittal J. Residue-specific α-helix propensities from molecular simulation. Biophys J. 2012;102:1462–7.

27. Piana S. A bias-exchange approach to protein folding. J Phys Chem B. 2007;111:4553-4559.

28. Tribello GA, Bonomi M, Branduardi D, Camilloni C, Bussi G. PLUMED 2: New feathers for an old bird. Computer Physics Communications. 2014 ;185:604–13.

29. Pietrucci F, Laio A. A Collective Variable for the Efficient Exploration of Protein Beta-Sheet Structures: Application to SH3 and GB1. J. Chem. Theo.

Comp. 2009;5:2197–201.

30. Greenfield N, Fasman GD. Computed circular dichroism spectra for the evaluation of protein conformation. Biochemistry. 1969;8:4108–16.

31. Frishman D, Argos P. STRIDE: Protein secondary structure assignment from atomic coordinates. Proteins 1995;23:455–79.

32. Shen Y, Bax A. Protein backbone chemical shifts predicted from searching a database for torsion angle and sequence homology. J Biomol NMR. 2007;38:289–302.

33. Zimm BH, Bragg JK. Theory of the Phase Transition between Helix and Random Coil in Polypeptide Chains. J. Chem. Phys. 1959;31:526–35.

34. Fersht AR. *Structure and mechanism in protein science.* W. H. Freeman and Co; 2002.

35. Tanford C. Protein denaturation. C. Theoretical models for the mechanism of denaturation. Adv Protein Chem. 1970;24:1–95.

36. Hoepfner V, Deringer VL, Dronskowski R. Hydrogen-bonding networks from first-principles: exploring the guanidine crystal. J Phys Chem A. 2012 10;116:4551–9.

Figures

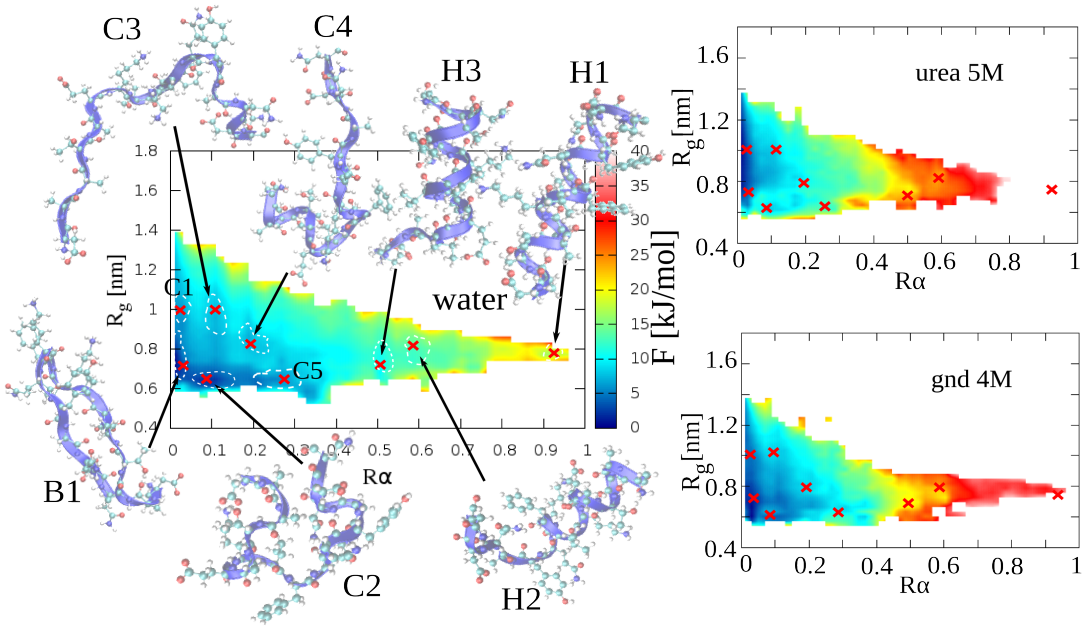

Figure 1: The free energy of the helix in water, 5M urea and 4M GndCl, as a function of the degree Rα of helix formation and of the gyration radius R_g. Different states identified for the peptide in water are marked with a cross in the plot, they are labelled with H1, H2, H3 (different degree of formation of the helix), C1, C2, C3, C4, C5 (coils) and B1 (hairpin), and their mean structure is shown. The crosses are reported also in the free-energy plots of the urea and GndCl simulations, for comparison. The dashed lines indicate isoenergetic curves at 2.5 kJ/mol above each minimum.

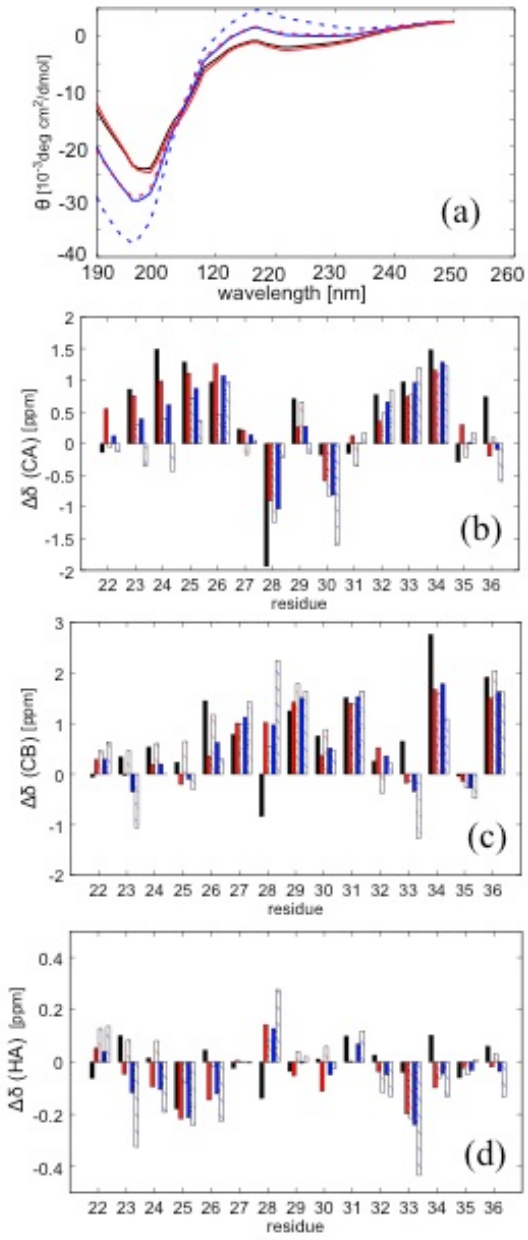

Figure 2: Circular dichroism (top plot) and chemical shifts of CA, CB and HA atoms (other plots) predicted from the model in water (black curves), 2M urea (solid blue curves), 5M urea (blue dashed curves), 2M GndCl (solid red curves) and 4M GndCl (dashed red curves).

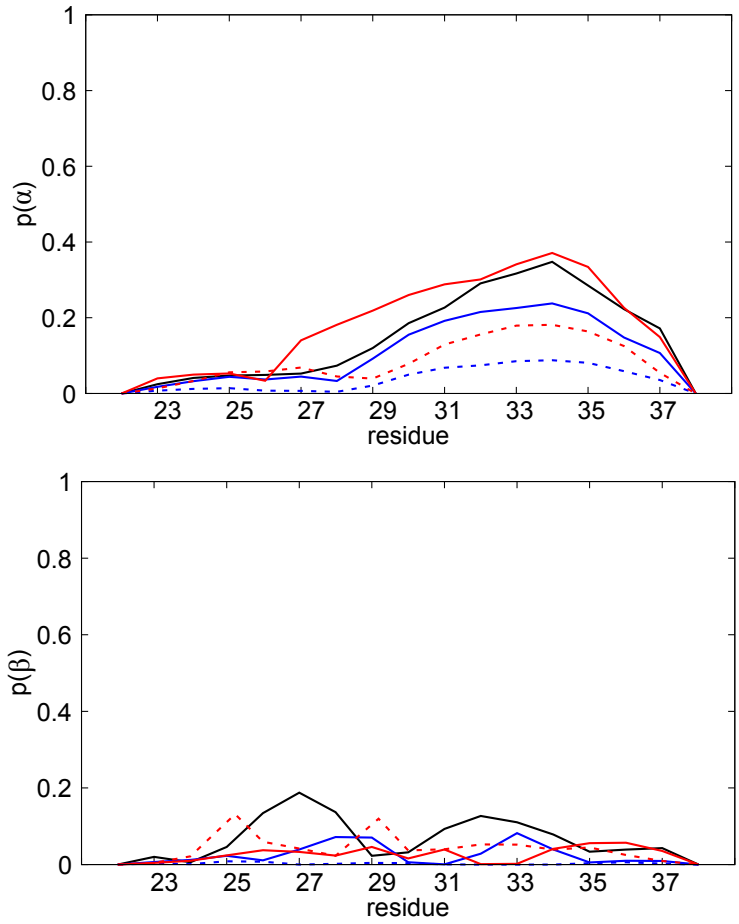

Figure 3: The probability of helical structures (above) and of extended beta structure (below) for each residue, calculated from the simulations in water (black curves), 2M urea (solid blue curves), 5M urea (blue dashed curves), 2M GndCl (solid red curves) and 4M GndCl (dashed red curves).

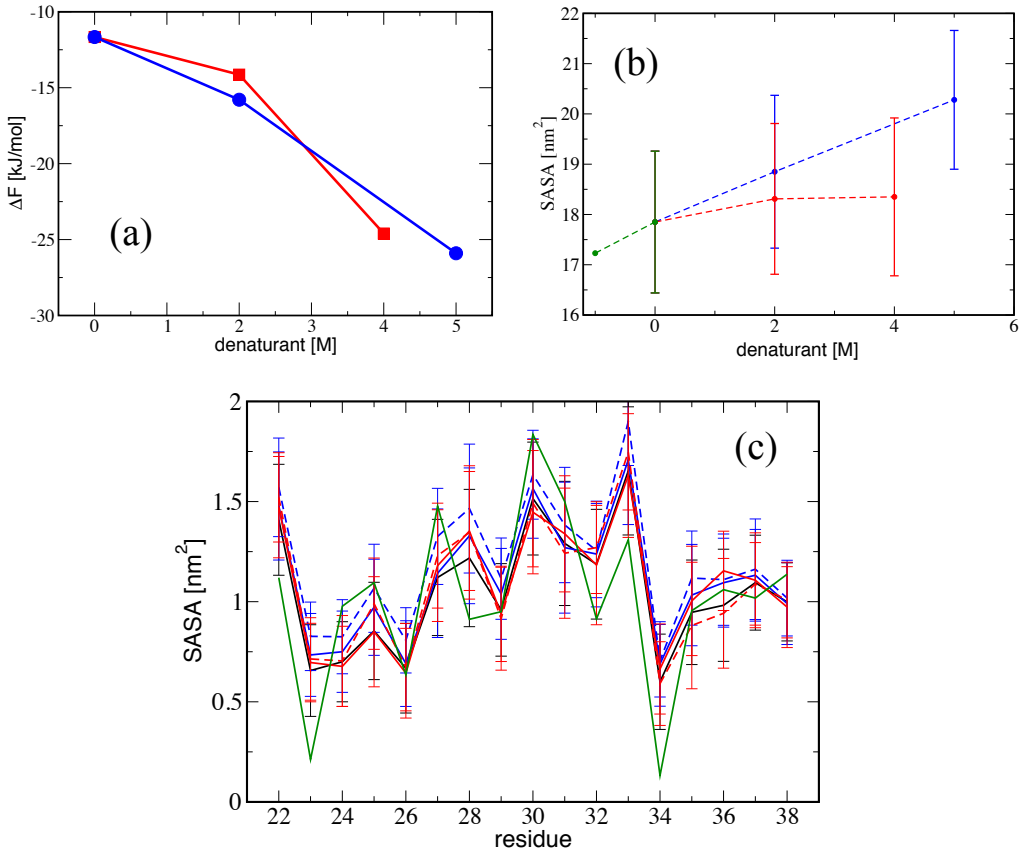

Figure 4: (a) The free energy difference ΔF as a function of the concentration of urea (in blue) and GndCl (in red). (b) The average surface area exposed to the solvent; the error bars indicate the fluctuations around the average; the green point indicate the value associated with the crystallographic structure of the helix within the native protein. (c) the exposed surface area per residue; the color code is the same as in Fig. 2; the green curve refers to the crystallographic structure.

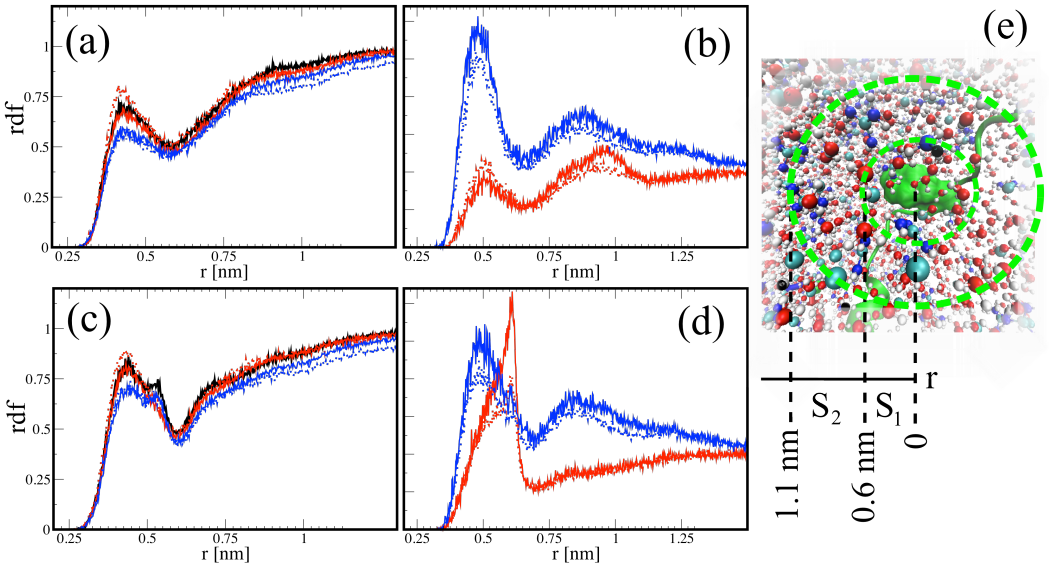

Figure 5: The radial distribution function of water (a, c) and of denaturant (b, d) around A26 (a,b) and E27 (c,d). A snapshot (e) of the helix in GndCl solution where the first shell S_1 and a larger neighborhood S_2 are marked with dashed lines.

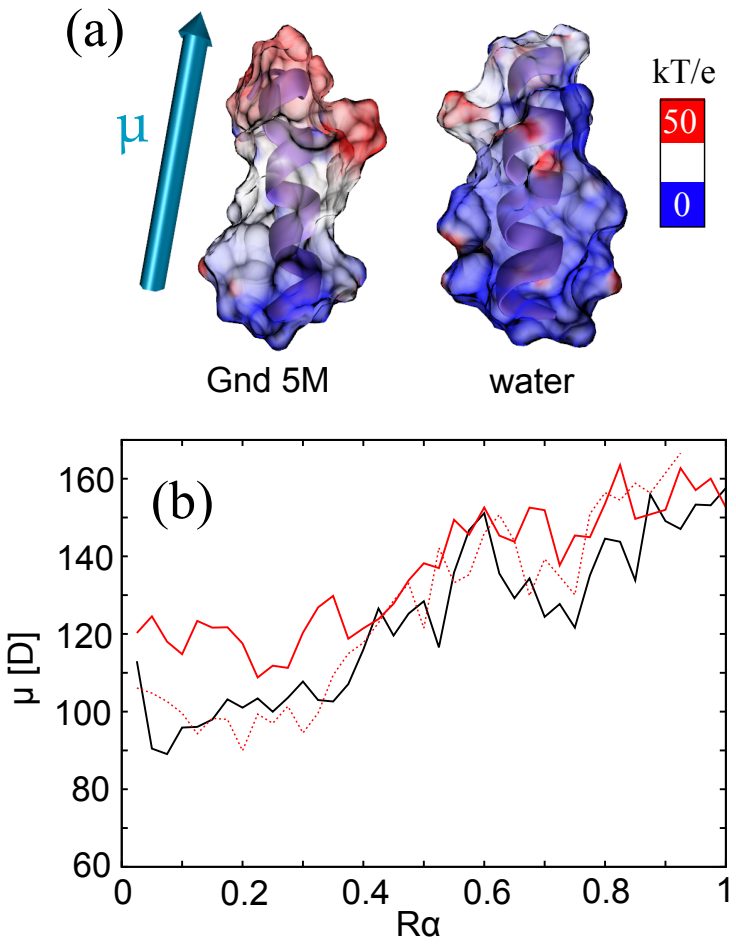

Figure 6: (a) The electric potential generated by the solvent on the surface of the native helix, obtained from the simulations in 5M GndCl (left panel) and in water (right panel). The colors range from blue, corresponding to a zero potential, to red, corresponding to 50 *kT/e*. (b) The dipole moment of the helix as a function of its degree of formation Rα.

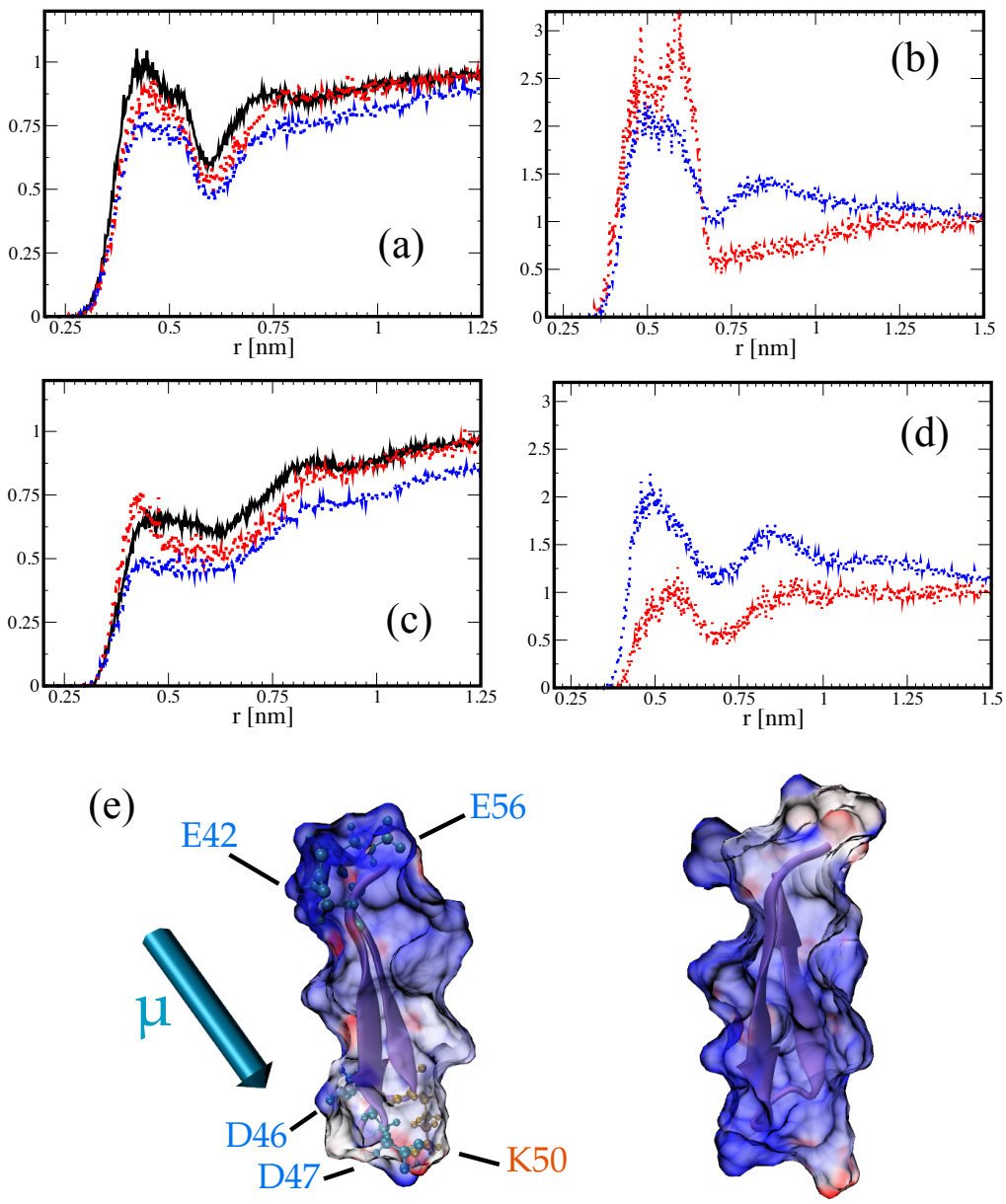

Figure 7: The rdf of water (a and c) and denaturant (b and d) around GLU42 (a and b) and THR49 (c and d). (e) The electric potential generated by GndCl on the surface of the hairpin, as in Fig. 6a.

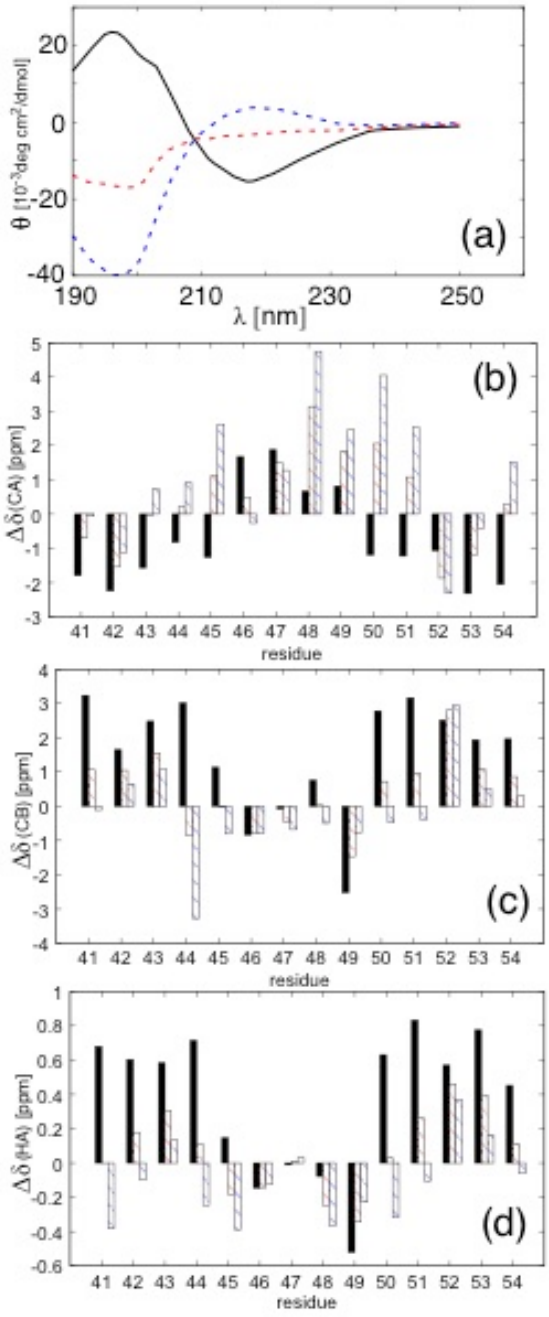

Figure 8: The Cd spectrum (a), the secondary chemical shifts of CA (b), of CM (c) and of HA (d) for the hairpin peptide in water (black curves), urea (blue curves) and GndCl (red curves).